Magnetic design optimization of the undulator for the VUV-FEL at the TESLA Test Facility

Yu.M.Nikitina*, J.Pflüger
Hamburger Synchrotronstrahlungslabor (HASYLAB)
at Deutsches Elektronen Synchrotron (DESY),
Notkestr. 85, 22603 Hamburg, Germany
(Permanent address: Department of Mathematical Physics*
Tomsk Polytechnical University , 634004 Tomsk, Russia)

January 16, 1996

Abstract

For the VUV-FEL at the TESLA Test Facility an undulator with superimposed strong focusing will be needed. A period length of 27.3 *mm*, a peak field of 0.5 *T* at a gap of 12 *mm* and a quadrupole gradient of about 20 *T/m* are required. In this report a magnetic design is presented which allows for these properties. Because it is a planar structure, it allows also for free access from the side for magnetic measurements and insertion of a vacuum chamber. In numerical calculations using the 3D code MAFIA the parameters for the magnet structure were optimized. Criteria for the selection of magnetic material are established. Forces acting on the magnetic components were calculated.

Introduction

At DESY in Hamburg a Free Electron Laser for the VUV spectral range at 6.4 *nm* using the principle of Self Amplified Spontaneous Emission is under construction [1]. It will use the electron beam of the TESLA Test Facility. The undulator at the TTF will have a total length of about 30 *m*. In order to keep the beam-size small over the whole undulator length an additional quadrupolar focusing is required. This can be realized by superimposing an alternating FODO lattice onto the undulator field. Fig.1 shows the schematic layout of the whole undulator section [1].

The magnetic array is subdivided into modules of 4.5 *m* length. There is a drift section of about 0.3 *m* between adjacent modules.

The undulator itself has two functions:

1. It has to provide the sinusoidal magnetic field so that the FEL process can take place.
2. It has to provide an alternating field gradient of about 20 *T/m*.

Using hybrid permanent magnet (PM) technology it is desirable to generate these fields in one magnetic arrangement. Five different types of focusing magnetic structures were studied numerically with help of 3-D code MAFIA.

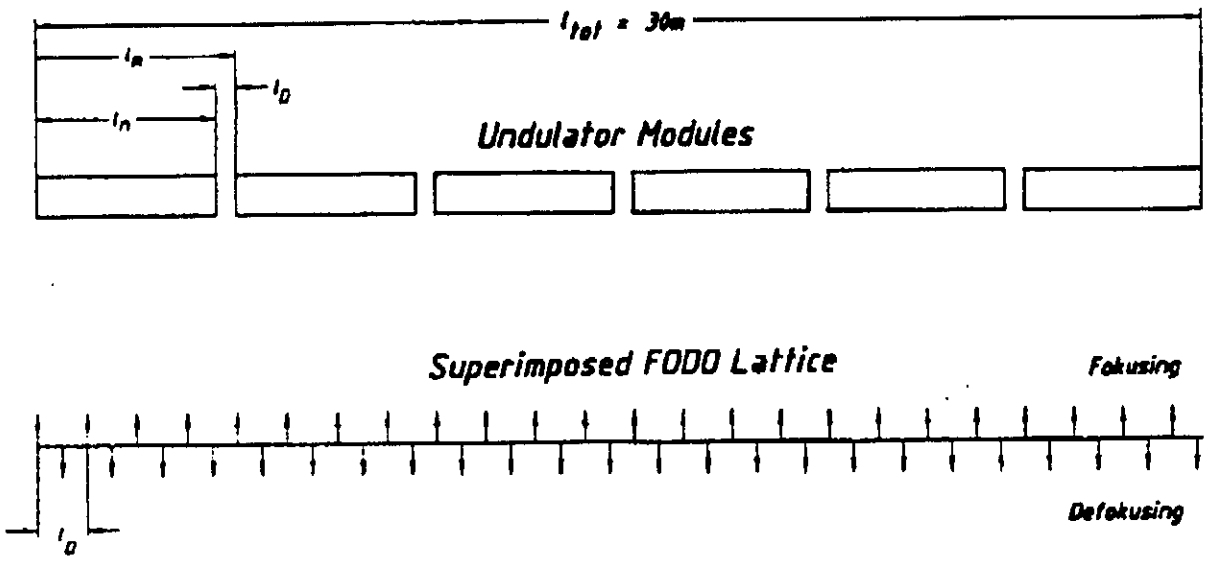

Figure 1: *General layout of the undulator for the VUV-FEl at the TESLA Test Facility.*

The detailed comparison is given in [2]. As a result of this investigation a novel focusing structure has been proposed.

1 Optimization of geometrical parameters of the structure

1.1 Proposed undulator design

To give a spatial impression of the proposed structure, Fig.2 shows one and a half period of the Four Magnets Focusing Undulator (4MFU) as described in detail in [3]. The magnets providing undulator field (magnetized along the z-axis) have been recessed by several millimeters so that there is now space for the focusing magnets, which are polarized parallel and anti-parallel along y, as can be seen in Fig.2. The structure satisfies all the requirements with respect to the gap, peak field and field gradient [3].

1.2 Choice of the main parameters

The parameters of the undulator which determine the optical properties were chosen on the basis of the following considerations [1, 4]:

1. The energy of the 1st harmonic should be 192 eV corresponding to 6.4 nm at an electron energy 1 GeV.
2. The K-parameter has to be larger than unity in order to keep the saturation length within an acceptable limit.

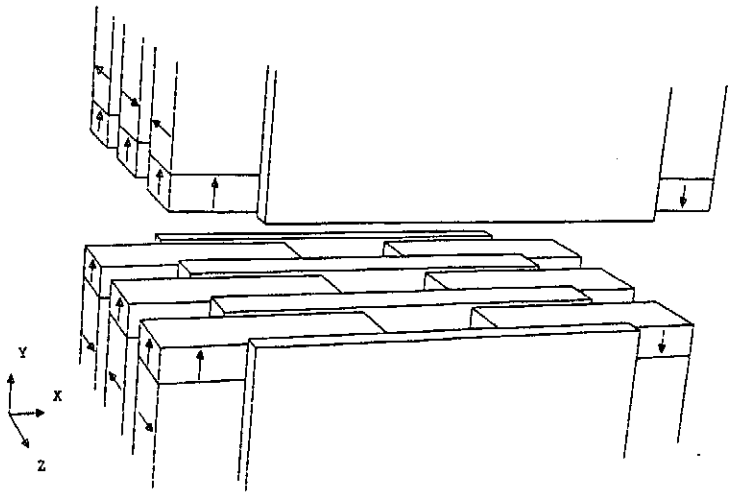

Figure 2: *3-D perspective view of the 1.5 periods of Four Magnets Focusing Undulator. The arrows indicate the directions of magnetization of the magnets.*

Undulator parameters	
Design gap	12 mm
Period length	27.3 mm
Peak field	0.5 T
K-parameter	1.27
Beam parameters	
Normalized emittance ε^n	$2\pi mrad\ mm$
Relative energy spread σ_E/E	0.1%
Peak current $\hat{I}$	2500 A
Radiation characteristics at 1.0 GeV	
γ	1956
Radiation wavelength	6.42 nm
Energy of the 1st harmonic	192 eV
Saturation length, $\beta = 3.0\ m$	24.96 m
Saturation power, $\beta = 3.0\ m$	1.49 GW

Table 1: *Summary of the main parameters of the undulator for the VUV-FEL at the TESLA Test Facility.*

In Table 1. the undulator parameters which fulfill these requirements are summarized. Saturation length and saturation power were calculated using the formulae of Kim and Xie [5].

1.3 Choice of materials

1. Poles

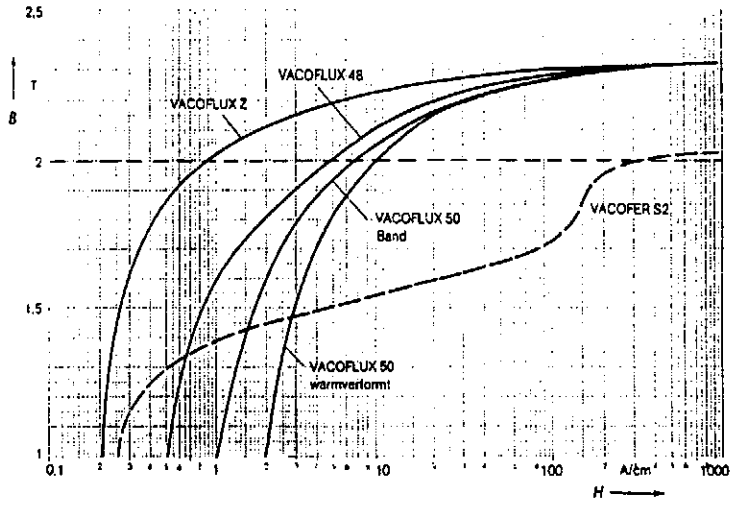

Figure 3: *The magnetization curves of different materials from Vacuumschmelze under the tradename Vacoflux. Dashed line indicates the region of interest in our case.*

The pole pieces in an undulator are usually operated at quite high field levels well above $2T$. Therefore cobalt iron which has a saturation density of about 2.3 T rather than conventional "soft iron" is used. Fig.3 shows the B-H curves from commercially available materials offered by Vacuumschmelze under the trade name "Vacoflux". The different curves correspond to different forms and heat treatments (thin metal sheets, solid bars, *etc.*). The curves differ at low H fields, but at higher H values the same saturation level of about 2.3 T is reached in all cases. It is well known that in order to increase performance at low H fields cobalt iron pieces need some heat treatment after machining. Since the field levels in the pole pieces near the gap are well above 2 T, the low field behavior of the different curves is only of minor importance. The Vacoflux50 "warmverformt" curve has been digitized for MAFIA program.

2. Magnets

NdFeB material is a magnet material with high remanent field and coercitive force. For all intents and purposes its B-H curve can be approximated by a straight line through $B = B_r$ at $H = 0$ and $B = 0$ at $H = -H_{CB}$. H_{CB} is the H-field at which the internal field B vanishes. Remanent magnetic field is B_r =1.2 T. The slope is given by the permeability which is μ =1.05 for NdFeB. The coercitive force of the material is assumed to be

large enough so that this approximation is valid. This condition can be met by proper material selection (see chapter 2).

1.4 Scope of parameter optimization

The goal of the parameter optimization was to select the geometrical parameters in such a way as to obtain optimum performance in terms of peak field and field gradient. Fig.4 shows two cross sections of the magnetic structure and also gives a definition of the important parameters used for the optimization.

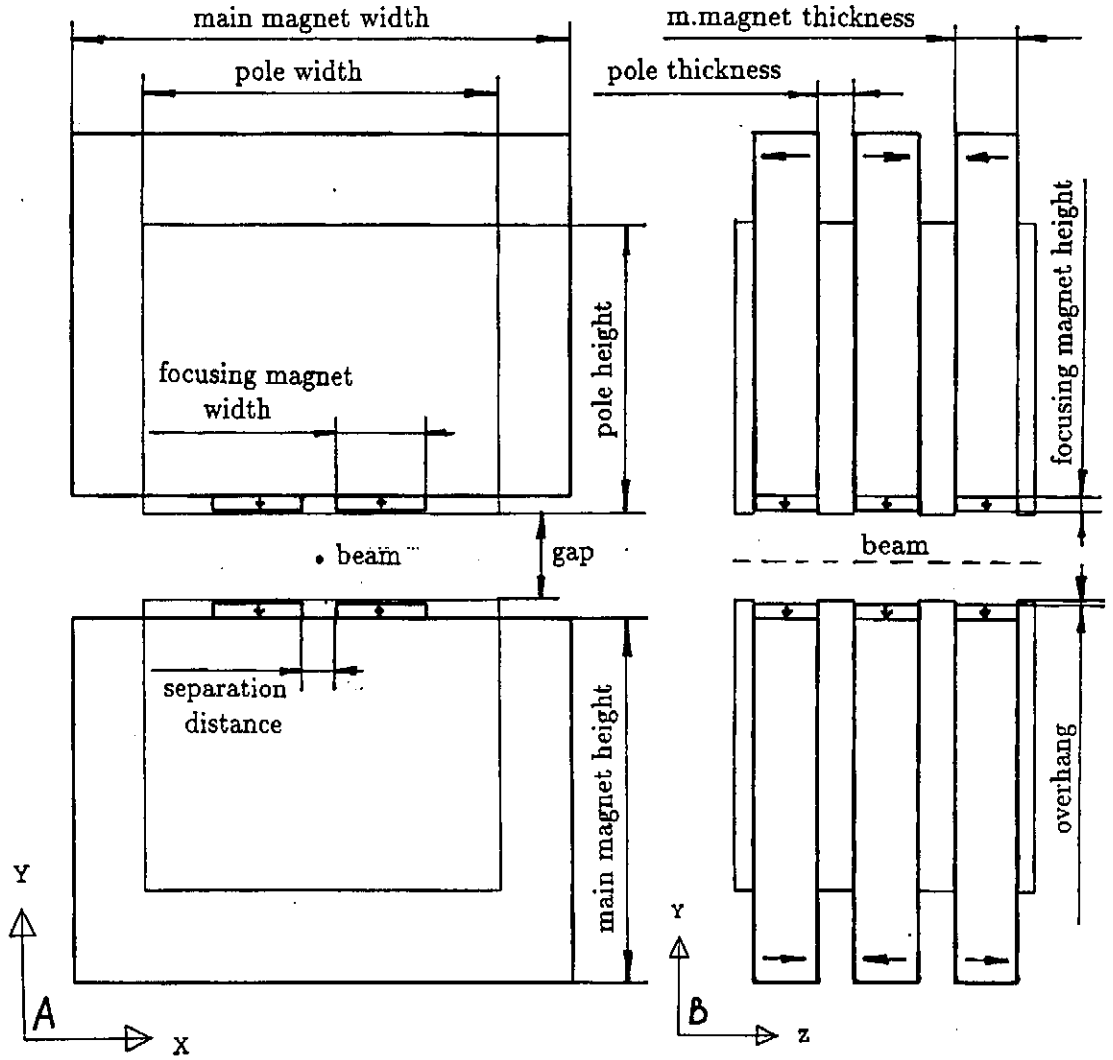

Figure 4: *A - crossection transverse to the beam direction, B - crossection parallel to the beam direction.*

All parameters are crosscorrelated with each other. As an example, the value of the average gradient strongly depends on the height of the focusing magnets. The thickness can be varied only in a very limited range and the influence of the width is almost negligible. Increasing the height of the focusing magnets can be achieved only at the expense of increasing the overhang of the

poles relative to the main magnets. But, the larger overhang of the poles causes stronger saturation and leads to a decrease of the peak field in the gap.

The aim of the optimization is to find the optimal relation between the height of the focusing magnets and overhang of the poles, which would give a peak field above 0.5 T and gradients over 20 T/m at the fixed period length of 27.3 mm and gap of 12 mm.

Parameter optimization

As a starting point the optimal pole thickness was selected, for a total overhang of only $0.5mm$, i.e. when no focusing magnets are present.

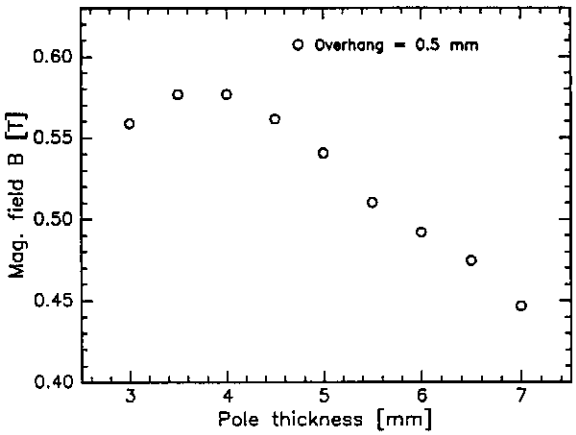

Figure 5: *Dependence of the peak field in the gap on the thickness of the poles.*

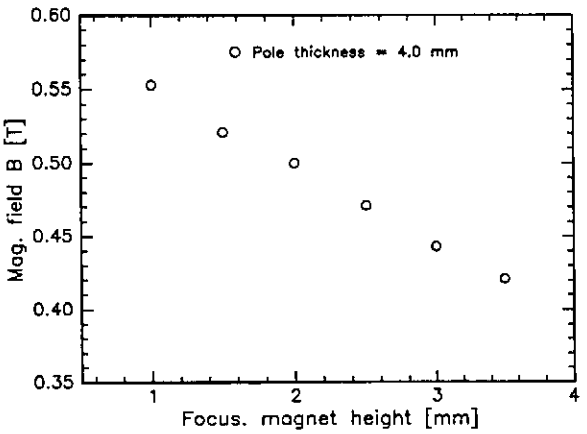

Figure 6: *Dependence of the peak field in the gap on the height of the focusing magnets.*

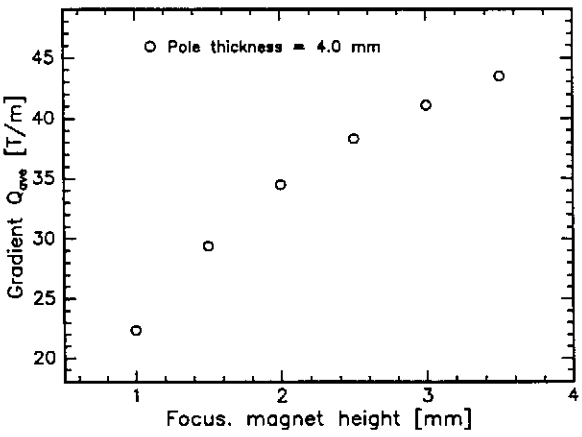

Figure 7: *Dependence of the gradient on the height of focusing magnets.*

Fig.5 shows the resulting magnetic field as a function of pole thickness. At the higher values of the pole thickness the peak field reduced due to the reduction of magnetic material. As the poles thickness is reduced, the volume of magnetic material increases and the peak field grows till it reaches the

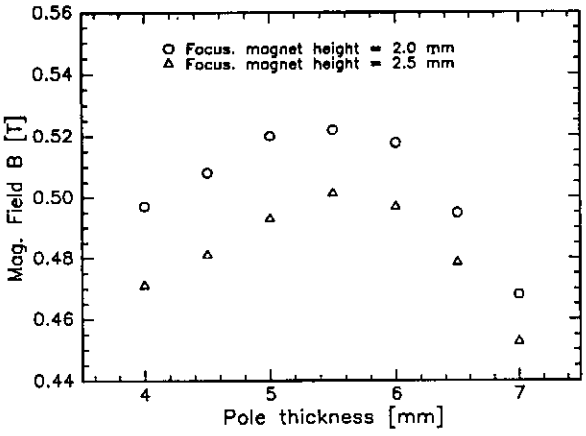

Figure 8: *Dependence of the peak field in the gap on the thickness of the poles for two different heights of the focusing magnets.*

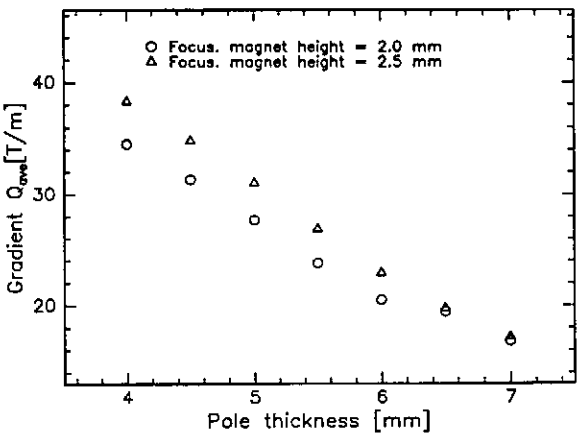

Figure 9: *Dependence of the gradient on the thickness of the poles for two different heights of the focusing magnets.*

maximum value of about 0.57 T at a pole thickness value of about $4mm$. A further decrease of pole thickness leads to strong saturation of poles and hence, the peak field decreases again. The optimal pole thickness of 4 mm was taken as a starting value for further optimization. It must also be mentioned, that the height of the poles and main magnets was chosen large enough, so that a change by several millimeters did not influence the peak field in the gap.

In order to gain space for the focusing magnets the total overhang has to be increased. The total overhang consists of the pole overhang of 0.5 mm plus the height of the focusing magnets. This will cause stronger pole saturation and a decrease of the peak field. Figs.6 and 7 show the dependence of the peak field and the corresponding gradient as a function of the height of focusing magnets.

It is seen that a focusing magnet height of $2mm$ results in a peak field of about 0.515 T which is already more than 10% less than the 0.57 T mentioned before. A field gradient of about 35 T/m can be reached in this way.

Fig.8 shows the recalculation analogous to Fig.5 for a focusing magnet heights of 2 and 2.5 mm with the overhang chosen appropriately. It is seen that due to the increased saturation the optimum is now around a pole thickness of 5 mm. Fig.9 shows the maximum field gradient for these two cases. The gradient strongly depends on the pole thickness. With increasing pole thickness it is reduced first due to reduced magnet length but also because poles are now less saturated. They are now a more effective magnetic shunt than in the saturated case.

Nevertheless, the average gradient is still 25.8 T/m at a pole thickness of $5mm$ and a focusing magnet height of $2.0mm$, which is sufficient for our purposes.

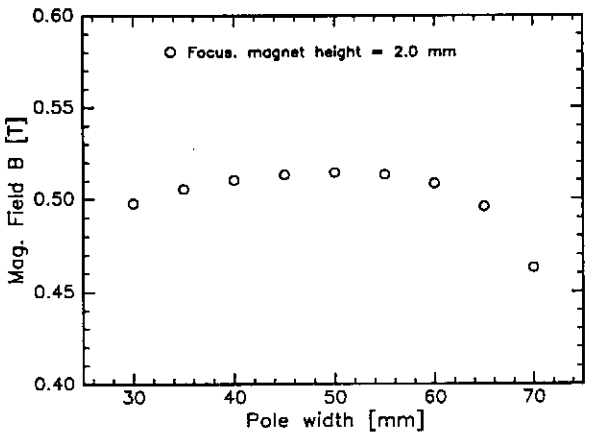

Figure 10: *Dependence of the peak field on the width of the poles.*

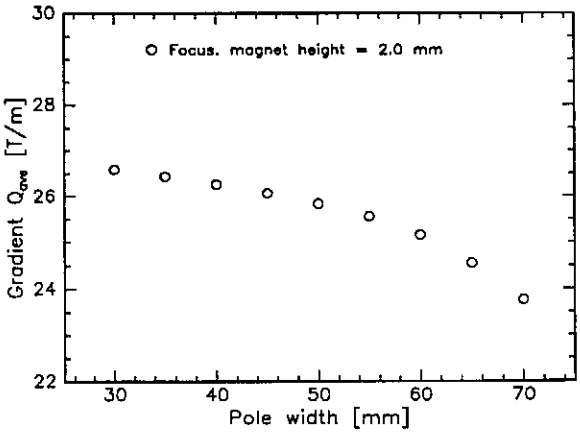

Figure 11: *Dependence of the gradient on the width of the poles.*

In Fig.10 the peak field as a function of the horizontal pole width is shown. It optimizes the overhang of the magnets in the horizontal direction. The optimal value of the pole width is 50 mm at the main magnet width of 70 mm. The dependence of the gradient is shown in Fig.11. It decreases monotonically with increasing width. However, the decrease is not large and can be tolerated.

The design of the 4MFU offers the possibility to adjust the gradient by changing the separation distance between the focusing magnets. This is an interesting feature for fine tuning of a magnet structure. Figs.12,13 show the peak field and the gradient as a function of the separation distance. An average gradient of 20 T/m can be achieved at a separation distance of about 4.3 mm as is shown in Fig.13. Fig.12 demonstrates an important property of the structure: The peak field on axis is completely independent of the separation distance and therefore independent of the gradient. This is important for building a structure with alternating gradients consisting of positive, zero and negative gradient sections.

1.5 Final results of parameter optimization

The final design parameters for the 4MFU are presented in Table 2.

The parameters listed in the Table 1 allow for obtaining the magnetic field with required properties:

1. The gradient of the quadrupolar field is in excess of the required 20 T/m. It can be adjusted by changing the separation distance between the focusing magnets. Tuning the separation distance down to zero will result in a gradient of 25.8 T/m.
2. The peak field is slightly above the required value of 0.5 T and does not depend on the separation distance between the focusing magnets.

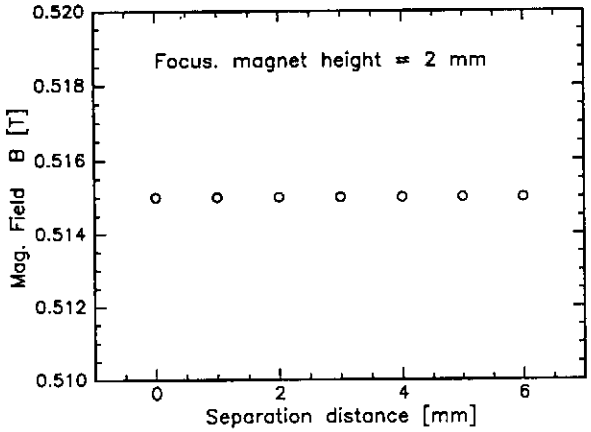

Figure 12: *Dependence of the peak field in the gap on the separation distance between the focusing magnets.*

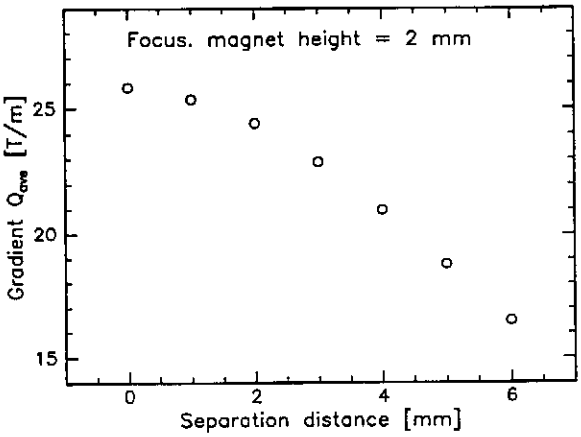

Figure 13: *Dependence of the gradient on the separation distance between the focusing magnets.*

Undulator parameters		
Period length λ		27.3 mm
Pole gap g		12 mm
Geometrical dimensions		
Main magnet	width	70 mm
	height	50 mm
	thickness	8.65 mm
Pole	width	50 mm
	height	40 mm
	thickness	5 mm
Focusing magnet	width	15 mm
	height	2 mm
	thickness	8.65 mm
result in		
Peak field B_{max}		0.515 T
Gradient Q_{ave}	max. at $d = 0.0$ mm	25.8 T/m
	req. at $d = 4.3$ mm	20 T/m

Table 2: *Optimized parameters for the 4MFU*

The focusing magnet array is very flexible. It is possible to have purely planar sections with and without focusing, the length of which have to be multiple of half the undulator period length.

2 Magnetization properties of materials

It is well known, that the relation between the external field H and the magnetic field B inside the permanent magnetic material in MKS units has the form:

$$\mu_0 H = B - M \tag{1}$$

where μ_0 is the permeability of the vacuum and M is the magnetization of the material. $M = B_r$ at $H = 0$.

Generally M is also dependent on H. For NdFeB this dependence is small up to about 90% of the H_{CM}, the H field at which the magnetization of the magnet vanishes. The external field H is also called demagnetizing field. Its direction inside magnetic material is opposite to the internal field B. Figs.14,15 give B(H) and M(H) curves for two magnet qualities commercially available from Vacuumschmelze. The curves are shown for a number of different temperatures. The material shown in Fig.14 (Vacodym362HR) has very high remanent field of about $1.35\,T$ at 20°C, but the behavior at even moderate demagnetizing field is poor, especially at elevated temperatures.

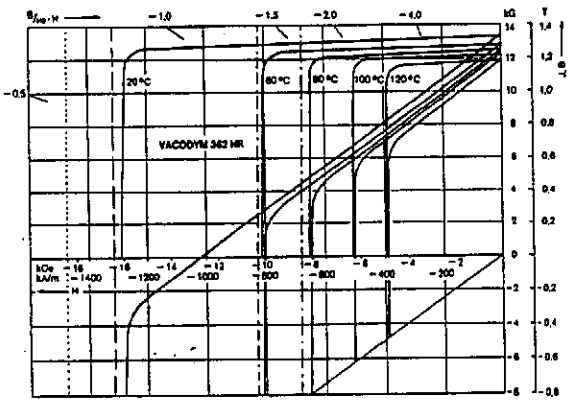

Figure 14: *Demagnetization curve of material VACODYM362 HR at different temperatures. The B(H) and M(H) curves are shown. Extremal working points are indicated by dots/dashes for main magnets, 'open gap'/'closed gap' and by dash-dash-dot/dot-dashed lines for the focusing magnets.*

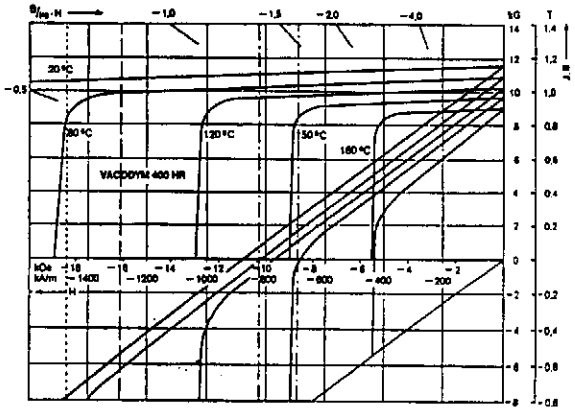

Figure 15: *Demagnetization curve of material VACODYM400 HR. the graphs and lines indicating extremal working conditions are the same as in Fig.14. The coercivity of this material is significantly increased.*

In contrast Fig.15 shows an alternative (Vacodym400HR) which has a somewhat lower remanent field but substantially better properties under demagnetizing fields.

In order to select a magnet material properly a detailed knowledge of the working point range of the magnetic material is essential. The field inside the magnetic material can be readily obtained from (1) assuming a constant magnetization of 1.2 T and using the numeric results from the MAFIA calculations.

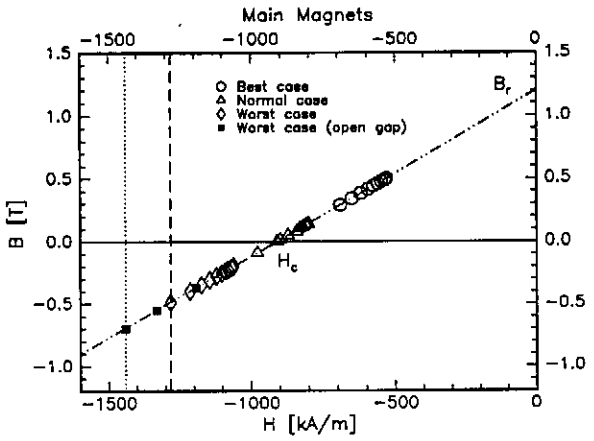

Figure 16: *BH-diagramm of the main magnets for three different locations inside the material. Dashed line indicates the worst working point.*

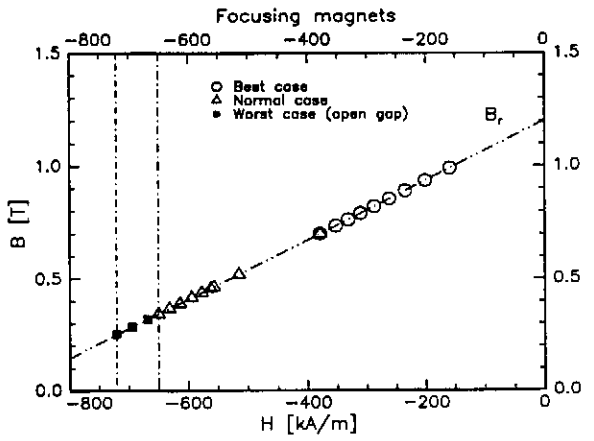

Figure 17: *BH-diagramm of the side magnets for two different locations inside the material. Dash-Dot line indicates the worst working point.*

Distinction has to made between 'open gap' condition which leads to higher demagnetizing fields and 'closed gap' condition. Fig.16 shows the result for the main magnets. The working point range extents to -1300 kA/m for 'closed gap' and to almost -1500 kA/m for 'open gap' condition. It is interesting to note that the points in Fig.16 show extreme cases which are located near the pole pieces. The average demagnetization is lower. Nevertheless, the extremal working conditions have to be considered for material selection. The 'closed gap' conditions are representative for routine operation of the device. For reasons of operational safety these working conditions have to be met at temperatures as high as 60°C. The 'open gap' conditions are representative for the assembling process where the upper and lower structure parts are not mounted together. Assembling however takes place under temperature controlled conditions at room temperature only. This relaxes the requirements on the magnet material since for the demagnetizing curves only room temperatures have to be considered.

Fig.17 shows the analogous data for the focusing magnets. Even at 'open gap' condition -750 kA/m is not exceeded. The working point ranges are shown in Fig.14 by additional lines. It is evident that a magnet material with properties like "Vacodym 400 HR" is required in order to avoid demagnetization losses.

3 Forces on materials

An important question for the mechanical design of the structure is the distribution of the magnetic forces acting between the parts of the undulator. The forces acting between the lower and upper structure parts can be estimated

by the total magnetic energy needed to fill out the volume between the low and upper parts of the undulator which is given by:

$$E_m = \frac{gw}{2\mu_0} \int B^2(z)dz$$

where g characterizes the vertical aperture (gap) and w is the horizontal width of the device, μ_0 is the permeability of the vacuum, B is the magnetic field along the undulator axis. It can be approximated by

$$B(z) = B_0 \sin(2\pi z/\lambda_0)$$

where B_0 is the peak field. The force is given by:

$$F = \frac{dE_m}{dg} = \frac{w}{2\mu_0} \int_z^{z+\lambda} B^2(z)dz' = \frac{w}{4\mu_0} B_0^2 \lambda$$

where

w	: 70. mm
B_0	: 0.5 T
λ	: 27.3 mm
μ_0	: 1.2566·10^{-6} Vs/Am

The parameters listed above result in $F = 95.0$ N per undulator period. The calculations with MAFIA gives the result $F = 75.0$ N. The difference is easily explained by the choice of the w. It characterizes the transverse region, within which the magnetic field stays homogeneous. For the calculations with analytical formula the total width of the undulator has been taken. It is clear, that the magnetic field is not homogeneous at the edges of the undulator any more.

Fig.18 shows the forces distribution between the materials as calculated by MAFIA.

4 Summary

The results of the magnetic optimization can be summarized as follows:

1. The optimal geometrical parameters of the structure have been defined, which allow for obtaining the required field properties.
2. The diagrams of the range of the working points have been presented, which give the information needed for the choice of magnetic material.
3. The forces acting between the parts of the undulator were calculated for starting the construction of the structure.

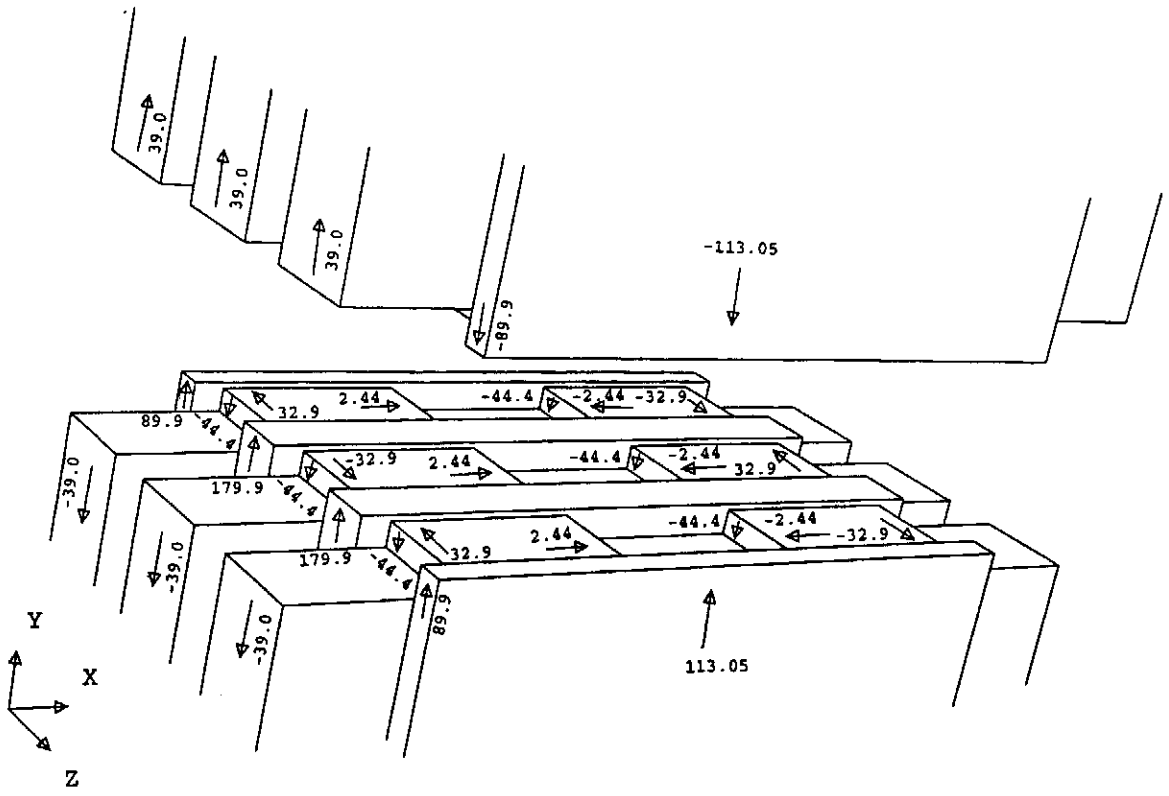

Figure 18: *Forces acting on materials (in Newton).*

This report sofar describes a novel type of undulator with strong focusing. Like for any other undulators a detailed consideration of required accuracies is needed before a mechanical design can be finished. These tolerance calculations will be subject to another publication.

References

[1] "A VUV Free Electron Laser at the TESLA Test Facility at DESY. Conceptual Design Report", DESY, TESLA-FEL 95-03, Hamburg, June, 1995.

[2] J.Pflüger, Yu.M.Nikitina, 'Undulator schemes with focusing properties for the VUV-FEL at the TESLA Test Facility', to be published in Nucl.Inst. and Meth.

[3] Yu.M.Nikitina, J.Pflüger, 'Two novel undulator schemes with quadrupolar focusing for the VUV-FEL at the TESLA Test Facility', Proceedings of the Conference 'FEL-95', New-York, August 1995, Nucl. Instr. and Meth. A, (in press)

[4] W. Brefeld, B. Faatz, Yu.M. Nikitina, J. Pflüger, P. Pierini, J. Roßbach, E.L. Saldin, E.A. Schneidmiller, M.V. Yurkov, 'Parameter study of the VUV-FEL at the TESLA Test Facility', Proceedings of the Conference 'FEL-95', New-York, August 1995, Nucl. Instr. and Meth. A, (in press)

[5] K.J. Kim, M.Xie Nucl.Instr. and Meth. A 331 (1993) 359